

Multi-frequency & Multi-epoch VLBI study of Cygnus A

U. Bach, M. Kadler, T.P. Krichbaum, E. Middelberg, W. Alef, A. Witzel and J.A. Zensus

Max-Planck-Institut für Radioastronomie, Auf dem Hügel 69, 53121 Bonn, Germany

Abstract. We present the first multi-frequency phase-referenced observations of Cygnus A done with the VLBA at 15 and 22 GHz. We find a pronounced two-sided jet structure, with a steep spectrum along the jet and a highly inverted spectrum towards the counter-jet. The inverted spectrum and the frequency dependent jet to counter-jet ratio suggest an obscuring torus in front of the counter-jet. From 14 epochs of 15 GHz VLBA data we accurately derive the jet and counter-jet kinematics. For the inner jet ($r \leq 5$ mas) we measure motions of $\beta_{\text{app}} \approx 0.2 - 0.5 h^{-1}$ and on the counter-jet side we find $\beta_{\text{app}} \approx 0.03 \pm 0.02 h^{-1}$. We discuss the jet velocities within the unified jet model.

1. Introduction

Cygnus A is one of the most powerful radio galaxies at a redshift of ($z = 0.057$). It is the archetypical FR II radio galaxy. In the radio bands, Cygnus A is characterized by two strong lobes separated by $\sim 2'$ in the sky. Two highly collimated jets connect the lobes with the core (Perley et al. 1984; Carilli et al. 1991). On kiloparsec scales, the jet is oriented along P.A. $\sim 285^\circ$ and the fainter counter-jet along P.A. $\sim 107^\circ$. Due to the large inclination of the jet with respect to the observer, and the correspondingly reduced relativistic effects, Cygnus A is an ideal candidate for detailed studies of its jet physics, which is thought to be similar to those of luminous quasars (e.g. Barthel 1989).

We present and discuss results from multi-frequency VLBI observations at 15, 22 and 43 GHz and from the first multi-frequency phase referenced observations of Cygnus A done with the VLBA at 15 and 22 GHz. To complement our data at 15 GHz we used ten epochs from the VLBA 2 cm Survey (Kellermann et al. 1998; Zensus et al. 2002) to analyse the source kinematics with improved accuracy.

2. Observations and Data Reduction

We observed Cygnus A in 1996 with the VLBA+Effelsberg at 15, 22, and 43 GHz, in 2002 at 5 and 15 GHz and in 2003 with the VLBA only at 15 and 22 GHz in phase-referencing mode. All observations were done in dual circular polarization and were correlated in Socorro. The data were reduced in the standard manner

using AIPS. The imaging of the source implying phase and amplitude self-calibration was done using DIFMAP.

After imaging we fitted circular Gaussian components to the self-calibrated data in order to parameterise the source structure. Conservatively, we assume errors of $\leq 10\%$ in the flux density arising from the uncertainties of the amplitude calibration and from the formal errors of the model fits. An estimate for the position error is given by $\Delta r = \frac{\sigma \cdot \Theta}{2S_p}$ (Fomalont 1989), where σ is the residual noise of the map after the subtraction of the model, Θ the width of the component, and S_p the peak flux density. This formula tends to underestimate the error if the peak flux density is very high or the width of the component is small. In the case of a small FWHM we used the beam size instead.

3. Results and Discussion

To investigate the spectral properties and the kinematics of Cygnus A on parsec scales we cross-identified individual model components along the jet using their relative separation from each other, their flux density and size. Since the observations from 2003 were phase-referenced, we compared the alignment between the two frequencies from the model fits with those from the phase-referencing and found similar results. The most likely position for the central engine is located between component C3 and J10 (see Fig. 1). This position shows a slightly inverted spectrum and turned out to be stable in our kinematical study. It seems to be the same position, which Krichbaum et al. (1998) already used in their study.

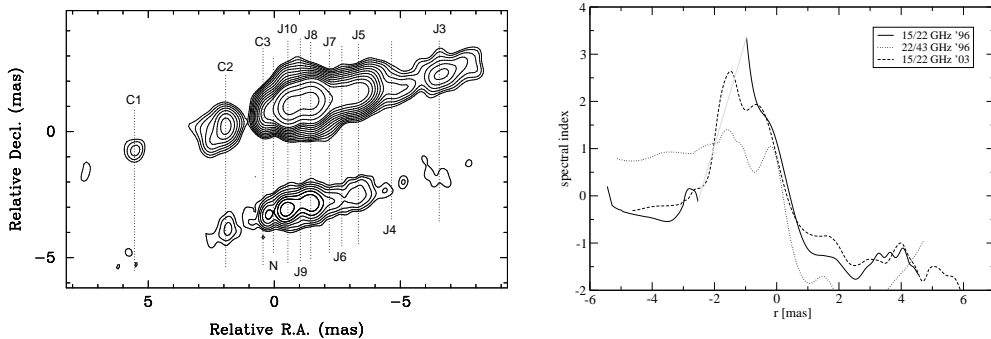


Figure 1. Left: Phase referenced contour images of Cygnus A at 15 GHz (top) and 22 GHz (bottom). The dotted lines indicate the position of the model fit components. Right: Profile of the spectral indices along the jet axis, 15/22 GHz from 1996 and 2003 and 22/43 GHz from 1996. $r = 0$ corresponds to the position of N in the left panel.

3.1. Spectral analysis

Figure 1 (left) shows the hybrid maps at 15 and 22 GHz with the positions of the model fit components denoted by dotted lines. The images are registered using phase-referencing to the quasar 2005+403 at a distance of 1.5° . On the right

hand side the spectral indices between 15, 22 and 43 GHz are plotted versus the core distance, assuming N is the core.

Our analysis reveals that the core spectrum is slightly inverted with a spectral index of $\alpha_{15/22} \approx \alpha_{22/43} \approx 0.5$. The jet shows a steep spectrum with spectral indices of $\alpha_{15/22} \approx -0.5$ to $\alpha_{15/22} \approx -1.2$ and $\alpha_{22/43} \approx -1.5$. The counter-jet has a highly inverted spectrum with $\alpha_{15/22}$ up to 2.5 in the inner part ($r \leq 2$ mas) and a flat spectrum between 15 and 22 GHz further out. Between 22 and 43 GHz the counter-jet spectrum is inverted with a spectral index of $\alpha_{22/43} \approx 1$. The inverted spectrum on the counter-jet side is likely due to free-free absorption by a foreground absorber. This is supported by the spectral behavior of the jet to counter-jet flux density ratio (Krichbaum et al. 1998; Bach et al. 2002). UV spectroscopy (Antonucci et al. 1994) and optical spectro-polarimetry (Ogle et al. 1997) also show evidence for a hidden broad line region. According to the unified scheme, this is strong evidence for an obscuring torus around the central engine and is consistent with the results from 21 cm absorption line VLBI (Blanco & Conway 1996).

3.2. Kinematics and Geometry

Figure 2 shows the component positions against time after a careful identification and linear fits to those, yielding apparent velocities β_{app} as follows. On the jet side the components start with 0.1 mas yr^{-1} near the core and accelerate to 0.25 mas yr^{-1} at larger separations. In Cygnus A 1 mas corresponds to $0.8 h^{-1} \text{ pc}$ so that an apparent motion of 0.1 mas yr^{-1} corresponds to $\beta_{\text{app}} = 0.26 h^{-1}$.

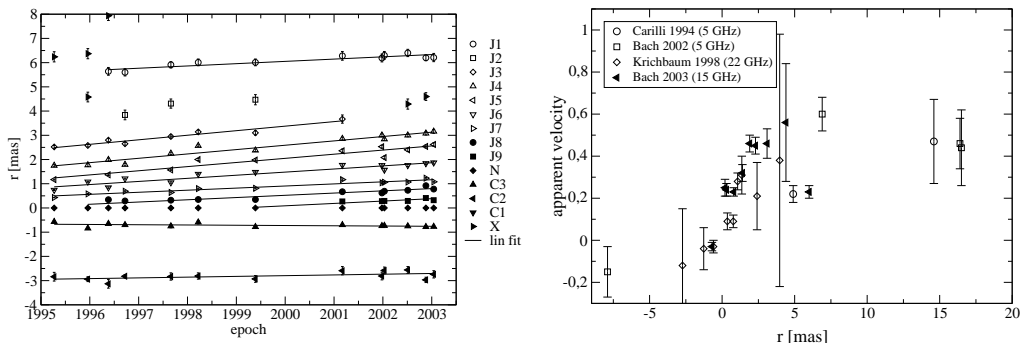


Figure 2. Left: Component distance at N versus time from 14 epochs of VLBI data at 15 GHz. Right: Apparent velocities versus separation from the core.

The situation on the counter-jet side is less clear than on the jet side. The components are weaker and more extended than on the jet side. The innermost component C3 shows a marginal motion of $0.010 \pm 0.007 \text{ mas yr}^{-1}$ and the next component C2 seems to travel inwards with $0.02 \pm 0.01 \text{ mas yr}^{-1}$. In the epochs with the highest quality data, component C2 consists of two nearly equally bright components. The apparent inward motion thus might be due to blending effects of these sub-components. A summary of the component speeds is given in Table 2. From the right panel in Fig. 2 it seems that the jet components accelerate as they travel down the jet and reach their maximum speed of $\sim 0.5 c$

Table 1. Proper motions of the jet and counter-jet components.

Comp	μ [mas/yr]	β_{app}	Comp	μ [mas/yr]	β_{app}
C2	0.02 ± 0.01	0.05 ± 0.03	J5	0.18 ± 0.01	0.46 ± 0.04
C3	-0.01 ± 0.01	-0.03 ± 0.02	J4	0.18 ± 0.02	0.45 ± 0.04
J9	0.10 ± 0.02	0.25 ± 0.04	J3	0.18 ± 0.03	0.46 ± 0.07
J8	0.09 ± 0.01	0.24 ± 0.03	J2	0.22 ± 0.11	0.56 ± 0.28
J7	0.09 ± 0.01	0.23 ± 0.02	J1	0.09 ± 0.01	0.23 ± 0.03
J6	0.13 ± 0.02	0.32 ± 0.04			

at a distance of $r \geq 2$ mas. Using $\beta_{\text{app}} = \frac{\beta \sin \theta}{1 - \beta \cos \theta}$, which is maximized at $\cot \theta = \beta_{\text{app}}$ and with $\beta_{\text{app}} = 0.5 h^{-1}$ one can calculate the lower limit of the intrinsic velocity β_{min} of $0.45 h^{-1} c$ and the corresponding angle to the line of sight of $\theta = 64^\circ$. Indeed, the analysis of the jet to counter-jet ratio also favors a large inclination of $80^\circ \pm 8^\circ$ (Krichbaum et al. 1998; Bach et al. 2002).

Due to the small relativistic effects at such conditions, the angle to the line of sight needs to change by more than 25° to explain the observed velocities by geometrical jet curvature. Since the jet appears to be very straight from parsec to kiloparsec scales, it is more likely that we observe a true acceleration, possibly caused by the collimation of the jet in the inner 2 parsec. Alternatively, we might observe a highly stratified jet with the different velocities belonging to different layers in the jet. This idea can also explain the absence of detectable motions on the counter-jet side. Due to the fact that we see the counter-jet from its ‘back’ the emission of the faster components is beamed away from us and we observe only the slower velocities of the outer sheath of the counter-jet.

Bach et al. (2002) detected apparent motion of $\beta_{\text{app}} = 0.15 \pm 0.12 h^{-1}$ on the counter-jet side at a distance of $r \approx 8$ mas from the core at 5 GHz, but this optically thin component is no more visible at 15 GHz. From the assumption of a simple Königl jet (Königl 1981) and an inclination of $65 - 80^\circ$ we would expect a proper motion of $\beta_{\text{app}} = 0.3 - 0.4 h^{-1}$ on the counter-jet side. That we do not see these ‘high’ velocities on the counter-jet points to a more complicated jet structure.

4. Conclusion

We carried out the first phase-referencing observations of Cygnus A with the VLBA at 15 and 22 GHz. The analysis of this data and a multi-frequency observation from 1996 at 15, 22 and 43 GHz revealed the spectral properties of the innermost jet structure in Cygnus A. We found a slightly inverted core and a steep jet spectrum. On the counter-jet side the inner part ($r \leq 2$ mas) shows a highly inverted spectrum with an $\alpha_{15/22}$ of up to 2.5 and $\alpha_{22/43} \approx 1$. In the outer regions the counter-jet shows a flat spectrum between 15 and 22 GHz and is still inverted between 22 and 43 GHz. Together with the frequency dependence of the jet to counter-jet ratio (Krichbaum et al. 1998; Bach et al. 2002) there is strong evidence that this is due to free-free absorption by an obscuring torus.

The apparent acceleration in the jet and the absence of detectable motions on the counter-jet side might reflect a more complicated jet structure than that

of the simple Königl jet with a well defined jet flow and questions the assumption that the jet and counter-jet are intrinsically the same. The observations could be explained by a stratification of the jet were we observe different velocities sheaths depending on the optical depth and the orientation of the jet.

Acknowledgments. We thank the group of the VLBA 2cm Survey for providing their data. This work made use of the VLBA, which is an instrument of the National Radio Astronomy Observatory, a facility of the National Science Foundation, operated under cooperative agreement by Associated Universities, Inc. and of the 100 m telescope at Effelsberg, which is operated by the Max-Planck-Institut für Radioastronomie in Bonn.

References

- Antonucci, R., Hurt, T., & Kinney, A. 1994, *Nature*, 371, 313
- Bach, U., et al. 2002, 6th EVN Symp., Bonn, ed. Ros E., (Bonn, MPIfR), 155
- Barthel P.D. 1989, *ApJ* 336, 606
- Blanco, P.R. & Conway, J. 1996, in *Cygnus A – Study of a Radio Galaxy*, ed. Carilli, C.L. & Harris, D.E., Cambridge University Press, 69
- Carilli C.L., Bartel N., & Linfield R.P. 1991, *AJ*, 102, 1691
- Fomalont, E.B. 1989 in *Synthesis Imaging in Radio Astronomy*, ASP Conf. Ser., Vol 6 Socorro, ed. Perley, R.A., Schwab, F.R. & Bridle, A.H., (San Francisco: ASP), 215
- Kellermann, K.I., et al. 1998, *AJ*, 115, 1295
- Königl, A. 1981, *ApJ*, 243, 700
- Krichbaum, T.P., et al. 1998, *A&A*, 329, 873
- Ogle, P.M., et al. 1997, *ApJ*, 482, L37
- Perley R.A., Dreher J.W. & Cowan J.J. 1984, *ApJ*, 285, L35.
- Zensus, J.A., et al. 2002, *AJ*, 124, 662